

WISE: Wavelet Transformation for Boosting Transformers’ Long Sequence Learning Ability

Yufan Zhuang¹ Zihan Wang¹ Fangbo Tao² Jingbo Shang¹

Abstract

Transformer and its variants are fundamental neural architectures in deep learning. Recent works show that learning attention in the Fourier space can improve the long sequence learning capability of Transformers. We argue that wavelet transform shall be a better choice because it captures both position and frequency information with a linear time complexity. Therefore, in this paper, we systematically study the synergy between wavelet transform and Transformers. Specifically, we focus on a new paradigm WISE, which replaces the attention in Transformers by (1) applying forward wavelet transform to project the input sequences to multi-resolution bases, (2) conducting non-linear transformations in the wavelet coefficient space, and (3) reconstructing the representation in input space via backward wavelet transform. Extensive experiments on the Long Range Arena benchmark demonstrate that learning attention in the wavelet space using either fixed or adaptive wavelets can consistently improve Transformer’s performance and also significantly outperform Fourier-based methods.

1. Introduction

Transformer (Vaswani et al., 2017) has become one of the most influential neural architectures in deep learning. Large pre-trained language models such as ChatGPT (OpenAI, 2023) and Galactica (Taylor et al., 2022) have reshaped people’s imagination of what an AI model can do in making conversation with humans, solving nontrivial math problems, writing code and even co-author a paper (Kung et al., 2022). In image processing, vision transformers have become the backbone for a wide range of applications (Dosovitskiy et al., 2020; Radford et al., 2021). On source code understanding, Codex (Chen et al., 2021a) can finish people’s code given the helper text of the function or just the

function name. All of those accomplishments are built upon the foundational Transformer. But the original design of the attention layer scales quadratically to the sequence length, becoming a scalability bottleneck of Transformers as texts, images, speech, and codes can be of vast lengths.

To remedy this, state-of-the-art attention methods have enabled Transformers to scale sub-quadratic or even linearly to the input sequence length. Typical approaches include using sparse attention patterns (Parmar et al., 2018; Wang et al., 2019; Beltagy et al., 2020; Zaheer et al., 2020), low-rank approximation (Wang et al., 2020; Chen et al., 2021b), and kernel approximation (Katharopoulos et al., 2020; Chormanski et al., 2020; Peng et al., 2020), where most of these methods are linear in time complexity. We refer readers to Section 4 for a comprehensive review.

Recent works on improving the effectiveness and efficiency of Transformers’ long-range capabilities start to explore attention learning in a transformed space. For example, conducting low-cost token-mixing with forward Fourier transform leads to remarkable accuracy improvement with a quasi-linear time complexity (Lee-Thorp et al., 2021). Token-mixing ideas (You et al., 2020; Lee-Thorp et al., 2021) are simple and effective, however, they lose Transformer’s universal approximating power by replacing attention with hard averaging (Yun et al., 2019). Moreover, without backward transform the model will mix information from both the input and transformed spaces, which is not mathematically sound. Since multiplication in the Fourier coefficient space, after projected back to the input space, is equivalent to directly convoluting in the input space, people have also utilized the forward and backward Fourier transform to learn large global filters with linear weights (Rao et al., 2021) and non-linearities (Guibas et al., 2021).

We propose Wavelet transformation for boosting Transformers’ long Sequence Learning (WISE) that facilitates the attention learning in a *wavelet coefficient space*, as shown in Figure 1(a). It requires only *linear time complexity* and keeps *universal approximating power*. Specifically, we first apply *forward* wavelet transform to project the input sequence to multi-resolution bases, then conduct non-linearity (e.g., full attention (Vaswani et al., 2017), random feature kernel (Rahimi & Recht, 2007)) in the wavelet coefficient

¹UC San Diego ²Mindverse.

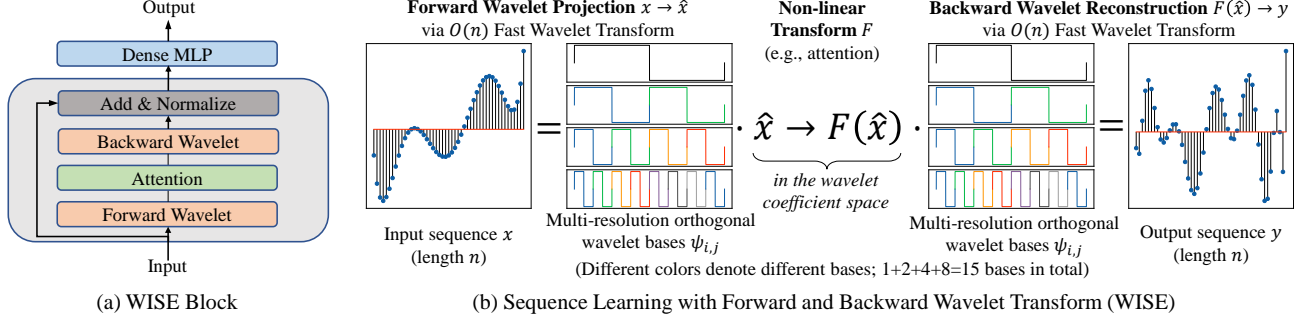


Figure 1: An overview of our proposed WISE. (a) The only difference between a Transformer block and a WISE block is the attention computation. (b) The general flow of computation in WISE with forward and backward wavelet transform.

space, and finally, reconstruct the representation in input space via *backward* wavelet transform. We name this general learning paradigm WISE, as shown in Figure 1(b), it can be suited with attention methods to boost their long-range learning capabilities. We implement wavelet transform using Fast Wavelet Transform (FWT) (Mallat, 1989) so both transform steps are linear in time. Intuitively, WISE operates on a local to global, coarse to fine-grained cascading structure. Compared with Fourier transform, wavelet transform is more efficient in time complexity and better captures local and positional information since the wavelet basis is localized in space with ranging granularity. Furthermore, we propose three ways to construct adaptive wavelets: direct wavelet parameterization, orthogonal wavelet parameterization, and wavelet lifting. We give detailed explanations of the three parameterization schemes and further discuss their individual advantages and drawbacks.

We conduct extensive experiments on the Long Range Arena (LRA) benchmark to empirically ablate and justify our proposed learning paradigm. When combined with various representative attention methods, WISE can boost their performance without incurring extra time complexities. We then analyze the performance of the three parameterization schemes when coupled with the attention methods, demonstrating even stronger performance boosts. This shows that learning in a wavelet coefficient space provides better long-range understanding capability than directly learning in the input space or in the Fourier space.

In summary, our major contributions are as follows.

- We propose WISE to facilitate learning in the wavelet coefficient space following a forward-backward paradigm which can be paired with attention methods and boost their long-range understanding capabilities.
- We further propose three adaptive wavelet parameterization schemes to maximize the flexibility of wavelet transformation.
- Extensive experiments on the Long-Range Arena benchmark have demonstrated the effectiveness and also justified the design of WISE.

2. Learning Attention in Wavelet Space

As shown in Figure 1(a), the only difference between a Transformer block and a WISE block is the attention computation. In this section, we introduce the details of moving the attention computation inside WISE. The general flow of WISE is shown in Figure 1(b), which constitutes the forward wavelet transform, the non-linearity (attention) in the middle, and the backward wavelet transform.

We list our notations here — we denote scalars as x , vectors as \mathbf{x} , matrices as X ; we denote function f 's transformation in the coefficient space as \hat{f} .

Background about Attention Let $X \in \mathbb{R}^{n \times d}$ denotes the input sequence of length n and hidden dimension d . A dense self-attention layer is shown below:

$$\text{Attention}(X) = \text{Softmax}\left(\frac{QK^\top}{\sqrt{d}}\right)V \quad (1)$$

where $Q = XW_q$, $K = XW_k$, $V = XW_v$ with $W_q, W_k, W_v \in \mathbb{R}^{d \times m}$ stand for the query, key, and value, respectively. The attention head size is denoted by m . The self-attention layer $\text{Attention}(\cdot)$ computes a weighted average for each column of V according to the dot-product similarity QK^\top that is of $O(mn^2)$ number of operations.

2.1. WISE Paradigm

We propose the WISE paradigm to conduct attention learning in the wavelet coefficient space between forward and backward transformation. The forward transformation, also called analysis, decomposes the input sequence into coefficients of a set of orthogonal, complete functional basis. We then conduct non-linear transformation in the coefficient space, which directly operates on the function. In the backward transformation, also called synthesis, we reconstruct the target representation in the original function space. With fixed wavelet families, we require the forward-backward transformation pair to be invertible and exact, meaning that one can perfectly reconstruct the same input from the coefficients.

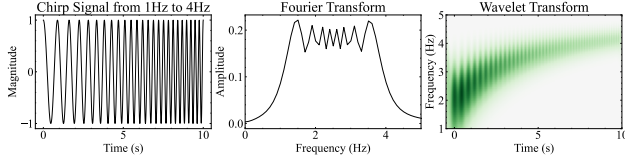


Figure 2: We show a chirp signal from 1Hz to 4Hz on the left, its Fourier transform in the middle and its wavelet transform on the right. As shown in the graph, from the Fourier transform graph one can only infer the existence of signal in the range of 1-4Hz without information on its happening time, while in the wavelet transform graph both time and frequency information are present and one can tell this is a chirp signal.

The general framework is shown below. Without loss of generality, we limit ourselves to 1d functions. Given input and output function $x(t), y(t) : \mathbb{R} \rightarrow \mathbb{R}$ on time domain t , functional basis $g(\omega, t)$ on both time domain t and frequency domain ω , and non-linear transformation F .

$$\text{Forward} \quad \hat{x}(\omega) = \sum_i x(t_i) g^*(\omega, t_i) \quad (2)$$

$$\text{Nonlinear} \quad \hat{h}(\omega) = F \circ \hat{x}(\omega) \quad (3)$$

$$\text{Backward} \quad y(t) = \sum_j \hat{h}(\omega_j) g(\omega_j, t) \quad (4)$$

where $g^*(\omega, t)$ denotes the complex conjugate of g in case g has complex parts.

As a concrete example, we use the well-known Fourier transformation pair (formula included in Appendix A.2) to illustrate this idea. Under Fourier transform, the functions are decomposed into sinusoidal waves, with $g(\omega, t) = e^{i2\pi\omega t}$. The coefficients will represent the magnitude of the corresponding sinusoidal function. Hence, learning the mapping between any sequential function $x(t) \rightarrow y(t)$ becomes learning a coefficient mapping between the transformed $\hat{x}(\omega) \rightarrow \hat{y}(\omega)$ in a vector space.

In WISE, we utilize the more localized wavelet transform as the forward-backward mechanism. We will explain the inner workings of our WISE's forward-backward transformation and the reason for choosing wavelet transform as the core in the next part.

2.2. Wavelet Transform

Fourier transform decomposes the entire function into global sinusoidal waves. It tells people what *frequencies* are there and in what *magnitude*, but no information is given about *when* that frequency started or ended. See Figure 2 for an illustration on a chirp signal. This limits the capability to understand the local structures of the input and to conduct

learning on top of it, which is crucial to many machine learning tasks.

Wavelet transform is designed to solve this issue. We give a basic introduction here, we refer interested readers to (Daubechies, 1992) for a more thorough explanation. Wavelet transform employs a function $\psi(x), x \in \mathbb{R}$, called mother wavelet, to generate a family of translated and dilated wavelets (see Figure 1(b)):

$$\psi_{i,j}(x) = 2^{\frac{i}{2}} \psi(2^i x - j), \quad i, j \in \mathbb{Z} \quad (5)$$

where scale i controls the resolution of the wavelet and j controls the position of the wavelet. With a larger i the wavelet will be squeezed shorter in space, hence the normalization factor $2^{\frac{i}{2}}$ to ensure the same L^2 norm for all wavelets. The wavelet family $\psi_{i,j}(x)$ is orthogonal on this dyadic grid.

To be a valid mother wavelet $\psi(x)$, the only requirement is admissibility:

$$\int_{\mathbb{R}} \psi(x) dx = 0 \quad (6)$$

In other words, the sum of function value should be 0.

Given any square integrable function $f \in \mathbb{L}^2(\mathbb{R})$ (i.e., $\int |f(x)|^2 dx < \infty$) and wavelet functions $\psi_{i,j}$, the wavelet transform pair is defined as:

$$\hat{f}(i, j) = \int_{\mathbb{R}} f(x) \psi_{i,j}^*(x) dx = \sum_t f(x_t) \psi_{i,j}^*(x_t) \quad (7)$$

$$f(x) = \sum_{i=-\infty}^{+\infty} \sum_{j=-\infty}^{+\infty} \hat{f}(i, j) \psi_{i,j}(x) \quad (8)$$

where $\psi_{i,j}^*(x)$ denotes the complex conjugate of $\psi_{i,j}(x)$.

Intuitively, in wavelet transform, we are scanning $f(x)$ with a microscope that has two knobs. One knob is the location j , the other one is the frequency (i.e., 2^i). We will be able to oversee the local structure of the input and calibrate it accordingly with parameterized functions in WISE paradigm.

To generalize beyond $\mathbb{L}^2(\mathbb{R})$ and avoid using an infinite number of wavelets, we must introduce another function ϕ , called scaling function with a similar admissibility and orthogonality constraint:

$$\int_{-\infty}^{+\infty} \phi(x) dx = 1, \quad \phi_{i,j}(x) = 2^{\frac{i}{2}} \phi(2^i x - j), \quad (9)$$

$$\text{s.t.} \quad \langle \phi_{i,j}, \psi_{i',j'} \rangle = 0, \quad i' > i, \quad \forall j, j'$$

$\phi_{i,j}$ is designed to cover the scale up to i , hence the orthogonality requirement. The decomposition of $f(x)$ therefore becomes:

$$f(x) = \sum_{j=-\infty}^{+\infty} \langle \phi_{0,j}, f \rangle \phi_{0,j}(x) + \sum_{i=0}^{+\infty} \sum_{j=-\infty}^{+\infty} \langle \psi_{i,j}, f \rangle \psi_{i,j}(x) \quad (10)$$

Note that although i still goes to $+\infty$ in (10), i usually has an upper limit in practice since it is impossible to work with infinite frequency. We also highlight that both the forward and backward discrete wavelet transform have an efficient $O(n)$ complexity algorithm (Mallat, 1989).

In the d -dimensional case, we do not have a general orthogonal discrete \mathbb{R}^d wavelet, unlike the continuous case. However, we can still perform discrete wavelet transform over each spatial dimension of the input, and we'd still be able to perfectly project and reconstruct the original function. To be more specific, for sequential inputs $X \in \mathbb{R}^{n,d}$ of length n and hidden dimension d , we will apply 2d wavelet transform over both the length and hidden dimension to generate the wavelet coefficients.

In a nutshell, wavelet transform enjoys $O(n)$ time complexity, an already desirable property compared to Fourier transform's $O(n \log n)$ complexity. It further provides the capacity to examine local structures with different resolutions via altering the scale. Learning carried out in this space will correspond to gathering and processing information from local to global, in a coarse to fine-grained fashion.

2.3. Direct Wavelet Parameterization

One key benefit of wavelet transformation is its flexibility in choosing the wavelets for its application, for example, Daubechies wavelets (Daubechies, 1992) are optimized to have the most compact support; symlet wavelets (Daubechies, 1988) are designed to have better symmetric properties. Therefore it is natural to consider parameterization of the wavelet coefficients and make wavelet transformation part of the learning process.

The direct parameterization scheme is the most intuitive approach. We make the wavelet coefficients learnable parameters, and update them during training. The key problem here is maintaining the structure between the scaling coefficients and the wavelet coefficients, i.e. the quadrature mirror filter (QMF) relationship (Daubechies, 1988). We consider parameterizing the scaling coefficients and expanding the system according to the QMF relationship to obtain the full set of wavelet coefficients, shown in equation 11.

$$\psi_{0,j} = (-1)^j \phi_{0,-j}, \quad j \in \mathbb{Z} \quad (11)$$

Further strengthening the learning power of adaptive parameterizations, we use different sets (i.e., d sets) of learnable wavelets for individual hidden dimensions of the input $X \in \mathbb{R}^{n,d}$. At the same time, we do not wish the output to have volatile changes when permuting the hidden dimensions. In other words, we want permutation invariance for the hidden dimensions. For that reason we only use 1d wavelet transform over the input's hidden dimension d for parameterized transformations, including this scheme and the following two parameterization schemes,

The direct parameterization scheme satisfies the QMF relationship automatically, but we have no guarantee that the trained wavelet will form an orthogonal wavelet basis. We enjoy more freedom at the cost of using a potentially imperfect projection and reconstruction pair.

2.4. Orthogonal Wavelet Parameterization

We provide another way to systematically construct parameterized orthogonal wavelets to keep the perfect reconstruction property intact. There exist extensive studies on this topic (Vaidyanathan & Hoang, 1988; Lina & Mayrand, 1993; Rieder et al., 1998; Neretti & Intrator, 2002), but many are based on constrained optimization, which is not ideal for our purpose. We present an unconstrained construction that originates from lattice filters, we refer readers to (Neretti & Intrator, 2002) for details of this design. In general, the orthogonal wavelets are constructed iteratively, each time we extend the wavelet by multiplying the current wavelet to an upshifted rotation matrix. The resulting wavelet basis will always be orthogonal, the formula is shown below:

$$\phi^{(n)} = R(\theta_1) \cdot U \cdot \dots \cdot U \cdot R(\theta_n) \quad (12)$$

where R is the rotation matrix and U is an upshift matrix.

As an example, we show how to construct a parameterized wavelet $\phi^{(4)}$ of length 4 from a parameterized wavelet of length 2 ($\phi^{(2)} = [\sin \theta_1, \cos \theta_1]$):

$$\begin{bmatrix} \phi_4^{(2)} \\ \phi_3^{(2)} \\ \phi_2^{(2)} \\ \phi_1^{(2)} \end{bmatrix} = \begin{bmatrix} \cos \theta_2 & 0 \\ -\sin \theta_2 & 0 \\ 0 & \sin \theta_2 \\ 0 & \cos \theta_2 \end{bmatrix} \begin{bmatrix} \sin \theta_1 \\ \cos \theta_1 \end{bmatrix} \quad (13)$$

θ_1, θ_2 represent the two rotation angles that we can set as learnable parameters.

This parameterization scheme offers naturally orthogonal wavelets without the need to customize the loss functions or derive a new optimization process. But on the other hand, this scheme requires more computation than the direct parameterization scheme and the compute cost grows with respect to the wavelet length.

2.5. Wavelet Lifting

The wavelet lifting scheme (Sweldens, 1998) is developed to become the second-generation wavelet transformation, due to its simplicity and extended flexibility. It is not characterized by transformation via functional convolution, rather it builds its forward and backward transformation from these three steps: 1. *segmentation*: splitting the input into two parts, one widely used segmentation is separating the even and odd parts of the input; 2. *update*: we mix the information from the subsampled segment into the wavelet segment

3. *lifting*: normalizing the subsampled segment and blend the information again.

The simplest design is the so-called Lazy wavelet (Sweldens, 1998; 1996), the forward transformation is shown below for the first level where $(\lambda_{1,:}, \gamma_{1,:})$ represent the subsampled coefficients and wavelet coefficients respectively:

$$\lambda_{1,k} = x_{2k}, \forall k \in \mathbb{Z} \quad (14)$$

$$\gamma_{1,k} = x_{2k+1} - \frac{1}{2}(\lambda_{1,k} + \lambda_{1,k+1}), \forall k \in \mathbb{Z} \quad (15)$$

$$\lambda_{1,k} = \lambda_{1,k} + \frac{1}{4}(\gamma_{1,k-1}, \gamma_{1,k}), \forall k \in \mathbb{Z} \quad (16)$$

It is assumed that each point in the input is related to its neighbors, hence in equation 15 we mix the information from the even segment to the odd segment. Then to make sure each decomposition level has the same mean and energy, we lift the subsampled coefficients with the wavelet coefficients, mixing the odd segment into the even segment in equation 16. In the Lazy wavelet lifting scheme, the wavelets are inexplicitly parameterized by non-linearities they are later applied to.

A second-level decomposition $(\lambda_{2,:}, \gamma_{2,:})$ will further decompose the $\lambda_{1,:}$ into finer-grained sequences. And the backward transformation is straightforward: simply reversing the positive and negative signs in the forward steps accordingly will recover the segments.

Wavelet lifting is a simple and straightforward alternative wavelet transformation scheme. The update and lifting step could be subject to arbitrary designs, which entitled this scheme with the most flexibility. However, what comes with this flexibility is the huge search space for finding the optimal lifting, hence we only use the basic Lazy wavelet in our study and leave the rest for future research.

2.6. Universal Approximation Power

In this subsection, we show that WISE can maintain the universal approximation power on seq-to-seq functions for Transformer and its variants. We illustrate this idea with proof for a slightly modified Performer (Choromanski et al., 2020) under WISE. The goal is to show that for any f in \mathcal{F} , $\forall p \in [1, +\infty), \forall \epsilon > 0$, we can find a \bar{f} in the class of WISE-Performer, such that:

$$d_p(f, \bar{f}) = \left(\int_{\mathbb{R}^n \times d} \|f(\mathbf{X}) - \bar{f}(\mathbf{X})\|_p^p d\mathbf{X} \right)^{\frac{1}{p}} \leq \epsilon$$

We define the WISE-Performer class that has positional encoding, h heads, head size s , hidden dimension r as $\mathcal{W}^{h,s,r}$ with FAVOR+ kernel with an additional normalization on the input.

Theorem 2.1. $\forall p \in [1, +\infty), \epsilon > 0$, and for any $f \in \mathcal{F}$,

we can find a WISE-Performer network $w \in \mathcal{W}^{2,1,4}$, such that $d_p(f, w) \leq \epsilon$.

The sketch of the proof is simple: since we have required the transformation pair to be invertible and exact, so for any seq-to-seq function, we can universally approximate it in the wavelet space and it is equivalent to having universal approximation power in the original space. The detailed proof of Theorem 2.1 is shown in appendix A.1.

3. Experiments

In this section, we first conduct experiments on the publicly available benchmark Long Range Arena (Tay et al., 2020b) to compare learning attention in the regular input space, in Fourier space with 2d Fourier transformation, and in wavelet space with fixed 2d Daubechies-2 wavelet transformation, demonstrating significant performance boosts (Table 1). We then analyze the performance of the three parameterization schemes when coupled with attention methods, showing even stronger performance boosts (Table 2). We also conduct ablation studies to validate the importance of backward reconstruction and the significance of wavelet initialization in the training. In the end, we provide an exploratory case study on the characteristics of the learned wavelets.

3.1. Experimental Design

Long Range Arena (LRA) LRA (Tay et al., 2020b) is designed to compare efficient transformers for their long-range reasoning ability. Since its release which already contains ten different efficient transformers, more and more efficient transformers have chosen it as the primary evaluation target. The datasets require understanding long sequences of mathematical operations, classifying text based on sentiment, matching similar documents, classifying images, and recognizing 2D spacial information. The sequence lengths of the dataset are within the range of 1K-4K.

Wavelet Transformation Details For fixed WISE, we use Daubechies-2 wavelet that has length 4 as the default choice and apply 2d wavelet transform with one decomposition level over both the sequence length and hidden dimension.

For adaptive WISE, we only transform over the sequence length axis because we intend to avoid large permutation variance over the hidden dimensions since we enabled learning distinctive adaptive wavelets over them. In our experiments, for direct wavelet parameterization we initialize from Daubechies-20 wavelet that has length of 40 or Daubechies-8 wavelet that has length of 16, for orthogonal wavelet parameterization we set the wavelet length as 16, for wavelet lifting we conduct three levels of decomposition. The detailed hyper-parameters are reported in Appendix A.3.

Table 1: Performance comparison of Transformers on Long Range Arena: Transformed space vs. Original space. We use \mathcal{F}/\mathcal{W} to denote that the attention is performed in the Fourier/wavelet space (which also adds an $O(n \log n)/O(n)$ complexity cost). We color the number green if it surpasses the baseline, red vice versa. [†] We reran Linformer & Linear Attention for all (N/A, \mathcal{F} , \mathcal{W}) with the same additional five sets of hyperparameters because of convergence issues. [‡] We note that we are unable to reproduce a score close to the original Linformer performance on Pathfinder. [§] This is the normalized version of Performer as described in Section 2.6.

Transformer Variants		ListOps			Text			Retrieval			Image			Pathfinder		
		N/A	\mathcal{F}	\mathcal{W}	N/A	\mathcal{F}	\mathcal{W}	N/A	\mathcal{F}	\mathcal{W}	N/A	\mathcal{F}	\mathcal{W}	N/A	\mathcal{F}	\mathcal{W}
Full	$O(n^2)$	36.37	17.80	37.15	64.27	56.42	74.82	57.46	51.78	72.43	42.44	31.41	42.29	71.40	50.55	78.25
Linformer	$O(n)$	35.70	36.15	37.65	53.94	57.06	55.22	52.27	55.93	65.85	38.47 [†]	34.89 [†]	39.17 [†]	66.44 [†]	61.76 [†]	70.21 [†]
Linear Att.	$O(n)$	16.13	37.65	37.55	65.90	71.66	71.93	53.09	72.71	70.71	42.32 [†]	51.07 [†]	40.83 [†]	75.91 [†]	70.45 [†]	76.43 [†]
Longformer	$O(n)$	35.63	18.95	36.65	62.85	55.36	74.99	56.89	52.52	66.21	42.22	29.12	37.10	69.71	50.38	78.15
Performer[§]	$O(n)$	18.01	37.15	38.20	65.40	65.52	75.60	53.82	60.56	78.56	42.77	9.99	42.98	77.05	50.49	79.17

Table 2: Evaluation results for the three adaptive parameterization schemes, we denote direct parameterization as AdaWISE, orthogonal parameterization as OrthoWISE, and wavelet lifting as LiftWISE.

Models	ListOps	Text	Retrieval	Image	Pathfinder
Transformer	36.37	64.27	57.46	42.44	71.40
AdaWISE	55.40	81.60	79.27	55.58	81.12
OrthoWISE	45.95	81.63	71.52	49.29	81.13
LiftWISE	42.95	75.63	56.45	42.48	81.73
Longformer	35.63	62.85	56.89	42.22	69.71
AdaWISE	49.30	79.73	58.57	50.84	79.48
OrthoWISE	39.45	78.41	79.93	49.93	79.47
LiftWISE	39.40	78.00	53.27	40.95	75.80
Linformer	35.70	53.94	52.27	38.47	66.44
AdaWISE	37.15	54.75	61.09	34.93	65.66
OrthoWISE	38.05	56.93	60.25	39.45	65.35
LiftWISE	37.30	54.43	70.73	34.66	63.49
Linear Att.	16.13	65.90	53.09	42.32	75.91
AdaWISE	38.90	76.82	71.38	54.81	79.68
OrthoWISE	39.55	79.45	69.65	49.93	78.09
LiftWISE	38.35	73.39	54.06	44.39	74.46
Performer	18.01	65.40	53.82	42.77	77.05
AdaWISE	46.05	80.93	71.16	52.06	77.17
OrthoWISE	39.80	79.10	57.67	48.78	78.09
LiftWISE	39.85	75.96	52.75	39.97	76.20

Experiment Environment. Our early-stage experiments are conducted on RTX 3090 GPUs and later moved to TPU v2-8s and v3-8s. Our code is written in Jax (Bradbury et al., 2018) with the Flax framework (Heek et al., 2020). The fixed wavelet transformation implementation is primarily based on Jax Wavelet Toolbox (Moritz Wolter, 2021) and PyWavelets (Lee et al., 2019).

3.2. Attention in WISE

Our WISE paradigm has a general philosophy of applying non-linearity in the wavelet space and is not limited to a certain type of attention method. We comprehensively evaluate representative attention methods on different space transformations (no transformation, 2d Fourier transformation, and 2d wavelet transformation with Daubechies-2 wavelet). We show that performing full attention, or many other at-

tention approximation operations in a wavelet transformed space as proposed in WISE paradigm almost always brings great accuracy improvements. In Table 1 almost all attention methods have increased accuracy when trained in the wavelet space compared to an untransformed space or the Fourier space, except for the Image dataset, where some incur a slight drop in accuracy.

We do note an interesting finding that Linear Attention (Katharopoulos et al., 2020) when coupled with a Fourier transformation space, showed pretty good results on all the tasks, and especially a significant improvement on the Image task¹. One hypothesis is that this is due to the fact that Linear Attention’s polynomial kernel in Fourier space, which occurs in the forms of $K(x, y) = (x^\top y)$, can be interpreted as self-convolution in input space. We leave this for future discovery.

3.3. Wavelet Parameterization Schemes

We demonstrate that the parameterized wavelets can further boost attention methods’ performance. In Table 2, we show results for the three parameterization schemes mentioned in Section 2 when each of these schemes is coupled with full attention and several other representative attention methods.

From the experiment results, we observe that direct parameterization almost always provides the highest accuracy elevation, followed by orthogonal parameterization and lifting. This is counter-intuitive: one would think imposing more structures should help the model to learn better wavelets, and in some cases it does, but our experiments show that learning wavelets with the most freedom is the best option most of the time. Does this mean wavelets’ nice mathematical properties are not essential at all, and any parameter initialization would work?

We conduct ablation studies where we initialize the directly parameterized wavelets from Gaussian distribution $N(\mu =$

¹Note that the hyperparameters were tuned for Linear Attention on this task, see Appendix A.3

0, $\sigma = 0.02$), and from damped sinusoidal waves ($x[t] = \frac{\cos(t)}{t+1}$). The results are shown in Appendix Table 8. This showcases the importance of initializing from wavelets even when we impose no constraints on them.

3.4. Exploratory Study on Learned Wavelets

Since we have trained the adaptive wavelet in the end-to-end fashion, we are naturally drawn to this question: what kind of wavelets has been learned? We use the best-performing direct parameterization scheme as an example, to empirically examine the learned wavelets.

We initiate our analysis from one commonly studied property of wavelets that characterizes the phase response of the wavelet (Rieder et al., 1998) – symmetry. A closer-to-symmetric wavelet (such as symlet) will have a closer-to-linear phase response, and a less symmetric wavelet (such as Daubechies) will have a more distorted phase response. We measure the symmetry by calculating the ℓ_1 norm between the unit-normalized wavelet and the wavelet’s transpose. A perfectly symmetric wavelet will have 0 on this measure.

From Figure 3, we observe that the variance in symmetry grows larger when going from shallow to deep layers. Also on average, the learned wavelets are almost always less symmetric compared to the Daubechies-20 wavelet. These results indicate that it is important to turn wavelet transformation into an adaptive process since the optimal wavelet design varies across the layers and the hidden dimensions.

3.5. AdaWISE-Atten

We compare the performance of our adaptive WISE when coupled with attention (AdaWISE-Atten) with other efficient transformers on the LRA benchmark in Appendix Table 5. When placed under WISE with adaptive wavelet, full attention automatically enjoys 2x speed-up with level 1 multi-resolution decomposition over the sequence length. The complexity will approach linear-time when the decomposition level goes higher. We show a significant performance boost when compared to other attention methods. Notably, our AdaWISE-Atten performed the best on four of the five datasets, and with a close-to-top performance on another, increasing full attention’s performance by 30%.

4. Related Work

4.1. Attention Methods

There has been plenty of prior work to enable transformers to handle long input more efficiently and effectively. Since the inefficiency comes from the quadratic dependency on sequence length because of the dense attention operation, a large portion of research simulates the attention operation with certain approximations, for example, replacing the

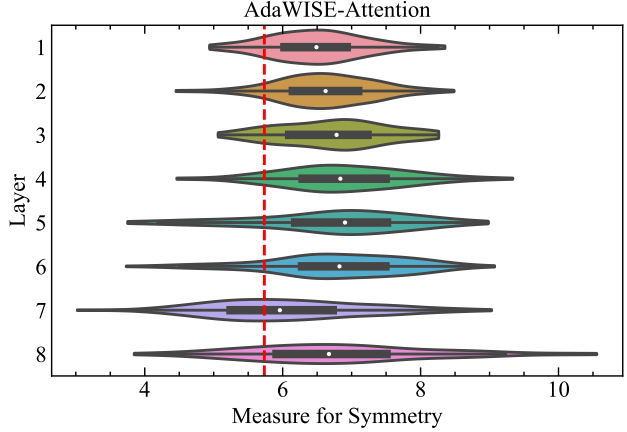


Figure 3: We show the measure for symmetry for all the layers of the AdaWISE-Attention trained on ListOps task. The density plot of each layer shows the distribution for all wavelets of each individual hidden dimension (in this case 128 wavelets). The red dotted vertical line denotes the measure for the Daubechies-20 wavelet, which is the wavelets’ initialization value.

dense attention matrix with a sparse version, or assume that it satisfies certain low-rank structures. We briefly review some methods on this topic in this section. For a more detailed survey, we refer the readers to Tay et al. (2020c).

Sparse Attention. Perhaps the most intuitive solution to alleviate the quadratic cost, Sparse Attention only calculates a portion of the full n^2 attention matrix. Early stage methods include Local Attention (Parmar et al., 2018) and Multi-passage BERT (Wang et al., 2019) use sliding windows or chunked blocks to speed up computation. Longformer (Beltagy et al., 2020) and BigBird (Zaheer et al., 2020) further combine global attention, sliding window attention, dilated sliding window attention, and random attention together to form strong sparse attention mechanisms, and BigBird showed that their method is a universal approximator of sequence functions. To make the block truncation a learnable process, Reformer (Kitaev et al., 2019) groups and sorts input segments via locality-sensitive hashing such that similar tokens are placed in the same chunk. Similarly, Sinkhorn Transformer (Tay et al., 2020a) trains a meta sorting network to reorganize input before applying windowed attention.

Low-rank Approximation. The self-attention matrix, at the center of transformer, has been found to display low-rank behaviors after pre-training. Linformer (Wang et al., 2020) performed spectrum analysis on the pre-trained attention matrix, and the results indicate that the top 128 singular values composite 88%-96% of the entire 512 singular values across attention heads and layers. Based on this observation, Linformer added low-rank projection matrices in attention to approximate the original attention matrix. On a similar notion, Drone (Chen et al., 2021b) extended the low-rank

approximation scope to all matrices in transformer via data-driven optimal compression.

Kernel Methods. The kernel methods approximate the whole self-attention by replacing the softmax with a kernel function that can be decomposed to avoid the explicit calculation of the $O(n^2)$ matrix multiplication. Linear Transformer (Katharopoulos et al., 2020) proposed a non-negative elu feature mapping as the substitution for the softmax, they further pointed out the connection between their formulation and RNNs, and argued that transformers and RNNs can be unified under the same umbrella. Building on top of this, Random Feature Attention (Peng et al., 2020) and Performer (Choromanski et al., 2020) utilized random feature approximation of the attention, one highlights the importance of normalization before random projection while the other one emphasizes the benefits of positive & orthogonal random features.

Token Mixing. Token Mixing methods are another version of efficient transformer building blocks. Different from the methods discussed above, they do not approximate attention, but rather conduct a new way of enabling communication between tokens. You et al. (2020) showed the possibility that a random token mixing strategy can work well in transformer encoders, as opposed to delicate (pre-)trained attention heads. Token Mixing is a new view towards self-attention as methods are not approximating self-attention. Lee-Thorp et al. (2021) pushed this idea further by providing an efficient method to mix the tokens with Fourier forward transformation.

Among these methods, our WISE utilizes wavelet transform, thus, is slightly similar to Token Mixing. However, our work should be seen as a new approach to boost transformers, which mixes the idea of an orthogonal space transform that communicates between tokens and attention methods that can benefit from the new space.

4.2. State Space Models

Different from all the attention methods, state space models (SSM) such as S4 (Gu et al., 2021) construct long-term memories utilizing orthogonal polynomial projection. They update and maintain the hidden states according to a differential equation, and output the states using linear projection. They have shown outstanding performance on LRA and other long-range tasks. It is also flexible in choosing the family of orthogonal polynomials, but for each polynomial family (Laguerre, Legendre) and each measure (uniform, truncated), significant effort is required to derive the explicit SSM formula. Similarly, MEGA (Ma et al., 2022) utilized the exponential moving average mechanism to construct its hidden space for recording long-range dependencies and has shown promising results. Our WISE is orthogonal towards the SSMs since our target is to boost attention methods'

performance on long-range tasks as a learning paradigm.

4.3. Fourier & Wavelet Transform in ML

Fast Fourier Transform (Cooley & Tukey, 1965) has been widely used in many machine learning domains, probably the most common usage is to speed up the computation of convolution. For a similar purpose to our work, AFNO (Guibas et al., 2021) learns global filters for images via adding block-wise MLP in Fourier transformation, equivalent to a convolutional layer with large filters. However, AFNO is designed for visual inputs, we show in our ablation study that such architecture cannot fully capture long-range text information.

Fast Wavelet Transform (Mallat, 1989) has been the backbone of numerous modern technologies including JPEG-2000 image compression (Skodras et al., 2001), digital communication (Akansu & Smith, 1995) and many others. FWT has been used for computation speed up (Wolter et al., 2020), speech recognition (Tufekci & Gowdy, 2000), and time series analysis (Michau et al., 2022). Recently in computer vision, WaveMix (Jeevan & Sethi, 2022) proposed to mix the input images with forward wavelet transform. We note that our work differs from theirs by learning the non-linear transformation in the coefficient space amid forward and backward wavelet transform.

5. Conclusions and Future Work

In this paper, we propose to learn attention in the wavelet coefficient space. Specifically, the inputs are first forward transformed into the wavelet space, then the attention is learned, and finally, we reconstruct the transformed sequence back in the input space. When coupled with attention methods, WISE can boost their performance on long-range understanding tasks while enjoying no extra cost in time complexity. We further propose three ways to learn adaptive wavelets: direct parameterization, orthogonal parameterization, and wavelet lifting. We discuss their advantages and drawbacks and evaluate them empirically. The experiments show adaptive wavelets can provide an even stronger lift to attention methods. In the end, we conduct an exploratory study on the learned wavelets' symmetric properties. The symmetry level varies across the layers, and the deeper layer tends to have greater variance, indicating the necessity of learning wavelets adaptively.

Through this work, we have focused on performing attention in the transformed wavelet space, either via fixed wavelet transformation or adaptive wavelet transformation. Is there an optimal way to construct learnable wavelets? And if so what should be the leading criterion for such optimality? These are both interesting questions we leave for the future.

Acknowledgements

Yufan Zhuang is supported by UC San Diego Jacobs School of Engineering Fellowship. We thank Sahil Suneja for valuable discussions.

References

- Akansu, A. N. and Smith, M. J. *Subband and wavelet transforms: design and applications*, volume 340. Springer Science & Business Media, 1995.
- Beltagy, I., Peters, M. E., and Cohan, A. Longformer: The long-document transformer. *arXiv preprint arXiv:2004.05150*, 2020.
- Bradbury, J., Frostig, R., Hawkins, P., Johnson, M. J., Leary, C., Maclaurin, D., Necula, G., Paszke, A., VanderPlas, J., Wanderman-Milne, S., and Zhang, Q. JAX: composable transformations of Python+NumPy programs, 2018. URL <http://github.com/google/jax>.
- Chen, M., Tworek, J., Jun, H., Yuan, Q., Pinto, H. P. d. O., Kaplan, J., Edwards, H., Burda, Y., Joseph, N., Brockman, G., et al. Evaluating large language models trained on code. *arXiv preprint arXiv:2107.03374*, 2021a.
- Chen, P., Yu, H.-F., Dhillion, I., and Hsieh, C.-J. Drone: Data-aware low-rank compression for large nlp models. *Advances in neural information processing systems*, 34: 29321–29334, 2021b.
- Choromanski, K. M., Likhoshesterov, V., Dohan, D., Song, X., Gane, A., Sarlos, T., Hawkins, P., Davis, J. Q., Mohiuddin, A., Kaiser, L., et al. Rethinking attention with performers. In *International Conference on Learning Representations*, 2020.
- Cooley, J. W. and Tukey, J. W. An algorithm for the machine calculation of complex fourier series. *Mathematics of computation*, 19(90):297–301, 1965.
- Daubechies, I. Orthonormal bases of compactly supported wavelets. *Communications on pure and applied mathematics*, 41(7):909–996, 1988.
- Daubechies, I. *Ten lectures on wavelets*. SIAM, 1992.
- Dosovitskiy, A., Beyer, L., Kolesnikov, A., Weissenborn, D., Zhai, X., Unterthiner, T., Dehghani, M., Minderer, M., Heigold, G., Gelly, S., et al. An image is worth 16x16 words: Transformers for image recognition at scale. *arXiv preprint arXiv:2010.11929*, 2020.
- Gu, A., Goel, K., and Re, C. Efficiently modeling long sequences with structured state spaces. In *International Conference on Learning Representations*, 2021.
- Guibas, J., Mardani, M., Li, Z., Tao, A., Anandkumar, A., and Catanzaro, B. Adaptive fourier neural operators: Efficient token mixers for transformers. *arXiv preprint arXiv:2111.13587*, 2021.
- Heek, J., Levskaya, A., Oliver, A., Ritter, M., Rondepierre, B., Steiner, A., and van Zee, M. Flax: A neural network library and ecosystem for JAX, 2020. URL <http://github.com/google/flax>.
- Jeevan, P. and Sethi, A. Wavemix: Resource-efficient token mixing for images. *arXiv preprint arXiv:2203.03689*, 2022.
- Katharopoulos, A., Vyas, A., Pappas, N., and Fleuret, F. Transformers are rnns: Fast autoregressive transformers with linear attention. In *International Conference on Machine Learning*, pp. 5156–5165. PMLR, 2020.
- Kitaev, N., Kaiser, L., and Levskaya, A. Reformer: The efficient transformer. In *International Conference on Learning Representations*, 2019.
- Kung, T. H., Cheatham, M., Medinilla, A., ChatGPT, Sillos, C., De Leon, L., Elepano, C., Madriaga, M., Aggabao, R., Diaz-Candido, G., et al. Performance of chatgpt on usml: Potential for ai-assisted medical education using large language models. *medRxiv*, pp. 2022–12, 2022.
- Lee, G. R., Gommers, R., Waselewski, F., Wohlfahrt, K., and O’Leary, A. Pywavelets: A python package for wavelet analysis. *Journal of Open Source Software*, 4(36): 1237, 2019. doi: 10.21105/joss.01237. URL <https://doi.org/10.21105/joss.01237>.
- Lee-Thorp, J., Ainslie, J., Eckstein, I., and Ontanon, S. Fnet: Mixing tokens with fourier transforms. *arXiv preprint arXiv:2105.03824*, 2021.
- Lina, J.-M. and Mayrand, M. Parametrizations for daubechies wavelets. *Physical Review E*, 48(6):R4160, 1993.
- Ma, X., Zhou, C., Kong, X., He, J., Gui, L., Neubig, G., May, J., and Zettlemoyer, L. Mega: moving average equipped gated attention. *arXiv preprint arXiv:2209.10655*, 2022.
- Mallat, S. G. A theory for multiresolution signal decomposition: the wavelet representation. *IEEE transactions on pattern analysis and machine intelligence*, 11(7):674–693, 1989.
- Michau, G., Frusque, G., and Fink, O. Fully learnable deep wavelet transform for unsupervised monitoring of high-frequency time series. *Proceedings of the National Academy of Sciences*, 119(8):e2106598119, 2022.

- Moritz Wolter. *Frequency Domain Methods in Recurrent Neural Networks for Sequential Data Processing*. PhD thesis, Rheinische Friedrich-Wilhelms-Universität Bonn, July 2021. URL <https://hdl.handle.net/20.500.11811/9245>.
- Neretti, N. and Intrator, N. An adaptive approach to wavelet filters design. In *Proceedings of the 12th IEEE Workshop on Neural Networks for Signal Processing*, pp. 317–326. IEEE, 2002.
- OpenAI. Chatgpt: Optimizing language models for dialogue, Jan 2023. URL <https://openai.com/blog/chatgpt/>.
- Parmar, N., Vaswani, A., Uszkoreit, J., Kaiser, L., Shazeer, N., Ku, A., and Tran, D. Image transformer. In *International conference on machine learning*, pp. 4055–4064. PMLR, 2018.
- Peng, H., Pappas, N., Yogatama, D., Schwartz, R., Smith, N., and Kong, L. Random feature attention. In *International Conference on Learning Representations*, 2020.
- Radford, A., Kim, J. W., Hallacy, C., Ramesh, A., Goh, G., Agarwal, S., Sastry, G., Askell, A., Mishkin, P., Clark, J., et al. Learning transferable visual models from natural language supervision. In *International Conference on Machine Learning*, pp. 8748–8763. PMLR, 2021.
- Rahimi, A. and Recht, B. Random features for large-scale kernel machines. *Advances in neural information processing systems*, 20, 2007.
- Rao, Y., Zhao, W., Zhu, Z., Lu, J., and Zhou, J. Global filter networks for image classification. *Advances in Neural Information Processing Systems*, 34:980–993, 2021.
- Rieder, P., Gotze, J., Nosse, J., and Burrus, C. S. Parameterization of orthogonal wavelet transforms and their implementation. *IEEE Transactions on Circuits and Systems II: Analog and Digital Signal Processing*, 45(2): 217–226, 1998.
- Skodras, A., Christopoulos, C., and Ebrahimi, T. The jpeg 2000 still image compression standard. *IEEE Signal processing magazine*, 18(5):36–58, 2001.
- Sweldens, W. Wavelets and the lifting scheme: A 5 minute tour. *ZAMM-Zeitschrift für Angewandte Mathematik und Mechanik*, 76(2):41–44, 1996.
- Sweldens, W. The lifting scheme: A construction of second generation wavelets. *SIAM journal on mathematical analysis*, 29(2):511–546, 1998.
- Tay, Y., Bahri, D., Yang, L., Metzler, D., and Juan, D.-C. Sparse sinkhorn attention. In *International Conference on Machine Learning*, pp. 9438–9447. PMLR, 2020a.
- Tay, Y., Dehghani, M., Abnar, S., Shen, Y., Bahri, D., Pham, P., Rao, J., Yang, L., Ruder, S., and Metzler, D. Long range arena: A benchmark for efficient transformers. In *International Conference on Learning Representations*, 2020b.
- Tay, Y., Dehghani, M., Bahri, D., and Metzler, D. Efficient transformers: A survey. *ACM Computing Surveys (CSUR)*, 2020c.
- Taylor, R., Kardas, M., Cucurull, G., Scialom, T., Hartshorn, A., Saravia, E., Poulton, A., Kerkez, V., and Stojnic, R. Galactica: A large language model for science. *arXiv preprint arXiv:2211.09085*, 2022.
- Tufekci, Z. and Gowdy, J. N. Feature extraction using discrete wavelet transform for speech recognition. In *Proceedings of the IEEE SoutheastCon 2000. 'Preparing for The New Millennium' (Cat. No. 00CH37105)*, pp. 116–123. IEEE, 2000.
- Vaidyanathan, P. P. and Hoang, P.-Q. Lattice structures for optimal design and robust implementation of two-channel perfect-reconstruction qmf banks. *IEEE Transactions on Acoustics, Speech, and Signal Processing*, 36(1):81–94, 1988.
- Vaswani, A., Shazeer, N., Parmar, N., Uszkoreit, J., Jones, L., Gomez, A. N., Kaiser, L., and Polosukhin, I. Attention is all you need. *Advances in neural information processing systems*, 30, 2017.
- Wang, S., Li, B. Z., Khabsa, M., Fang, H., and Ma, H. Linformer: Self-attention with linear complexity. *arXiv preprint arXiv:2006.04768*, 2020.
- Wang, Z., Ng, P., Ma, X., Nallapati, R., and Xiang, B. Multi-passage bert: A globally normalized bert model for open-domain question answering. In *Proceedings of the 2019 Conference on Empirical Methods in Natural Language Processing and the 9th International Joint Conference on Natural Language Processing (EMNLP-IJCNLP)*, pp. 5878–5882, 2019.
- Wolter, M., Lin, S., and Yao, A. Neural network compression via learnable wavelet transforms. In *International Conference on Artificial Neural Networks*, pp. 39–51. Springer, 2020.
- You, W., Sun, S., and Iyyer, M. Hard-coded gaussian attention for neural machine translation. In *Proceedings of the 58th Annual Meeting of the Association for Computational Linguistics*, pp. 7689–7700, 2020.
- Yun, C., Bhojanapalli, S., Rawat, A. S., Reddi, S., and Kumar, S. Are transformers universal approximators of sequence-to-sequence functions? In *International Conference on Learning Representations*, 2019.

Zaheer, M., Guruganesh, G., Dubey, K. A., Ainslie, J., Al-berti, C., Ontanon, S., Pham, P., Ravula, A., Wang, Q., Yang, L., et al. Big bird: Transformers for longer sequences. *Advances in Neural Information Processing Systems*, 33:17283–17297, 2020.

A. Appendix

A.1. Proof for Theorem 2.1

We define the function class \mathcal{F} to be the set of all countinous functions that map a compact domain in $\mathbb{R}^{n \times d}$ to $\mathbb{R}^{n \times d}$.

We start from making the connection between random feature kernel and regular transformer block:

Lemma A.1. (Asymptotic Result for FAVOR+) *The following is true for independent random w_i ,*

$$\begin{aligned} & \text{MSE}(\hat{\text{SM}}(x, y)) \\ &= \frac{1}{m} \exp(\|x + y\|^2) \text{SM}^2(x, y) (1 - \exp(-\|x + y\|^2)) \\ \Rightarrow & \lim_{\text{SM}(x, y) \rightarrow 0} \text{MSE}(\hat{\text{SM}}(x, y)) \rightarrow 0 \end{aligned}$$

where SM denotes the softmax kernel, $\hat{\text{SM}}$ denotes the random feature kernel, and MSE stands for mean-squared error.

The proof of this lemma can be found at [Choromanski et al. \(2020, Lemma 2\)](#). It tells us the the MSE error is upper bounded to a constant since x, y is normalized beforehand, and vanishes to 0 as the original softmax kernel value tends to 0 and the number of random features m tends to $+\infty$.

Next we use the main theorem of [Yun et al. \(2019\)](#). We denote the transformer network class that has positional encoding, h heads, head size s , and hidden dimension r as $\mathcal{T}^{h,s,r}$.

Lemma A.2. $\forall p \in [1, +\infty)$, $\epsilon > 0$, and for any $f \in \mathcal{F}$, we can find a Transformer network $g \in \mathcal{T}^{2,1,4}$, such that $d_p(f, g) \leq \epsilon$.

The proof of Lemma A.2 constitutes of several steps, of which the first step is to approximate any function $f \in \mathcal{F}$ as a piece-wise constant function \tilde{f} . Since f is continuous, the piece-wise constant approximation can be of arbitrary accuracy. Next they find a modified transformer \tilde{g} with hard-max operator and a special class of activations. Finally they show that the transformer block g is able to approximate \tilde{g} . The functional distance is then bounded by:

$$d_p(f, g) \leq d_p(f, \tilde{f}) + d_p(\tilde{f}, \tilde{g}) + d_p(\tilde{g}, g) \leq \epsilon$$

We show that with slight modification, the proof will work for WISE-Performer, and can be generalized to the WISE paradigm under certain constraints.

Hyperparameter	Config ₁	Config ₂	Config ₃	Config ₄	Config ₅
Layers	1	1	2	2	2
Embedding Dim.	128	128	128	256	256
Attention Dim.	64	64	64	64	64
MLP Dim.	128	128	256	1024	512
Attention Heads	8	8	2	4	4
Dropout	0.2	0.1	0.1	0.1	0.2
Attention Dropout	0.1	0.1	0.1	0.1	0.1

Table 3: Additional hyperparameter configurations tried for Linformer and Linear Trans. in Image and Pathfinder

The proof is outlined below: For $\forall f \in \mathcal{F}$, its wavelet transform \hat{f} (we will also use f_w to denote this, see (7) for details) is still continuous. Hence, the discretization claim remains valid. We can then effectively approximate the self-attention transformer block with the FAVOR+ block up to $\frac{\epsilon}{4}$ difference by controlling the number of random features m . In the end, the backward reconstruction is exact, the distance bound becomes when we control the other three terms to be less than $\frac{1}{4}\epsilon$ as well:

$$\begin{aligned} & d_p(f, w) \\ & \leq d_p(f_w, \tilde{f}_w) + d_p(\tilde{f}_w, \tilde{g}) + d_p(\tilde{g}, g) + d_p(g, w) \\ & \leq \epsilon \end{aligned} \quad \square$$

A.2. Fourier Transform Pair

Given function $f(x)$, $x \in \mathbb{R}$, the Fourier transform pair is defined as the following:

$$\text{Forward : } \hat{f}(\omega) = \int_{-\infty}^{\infty} f(x) e^{-i2\pi\omega x} dx \quad (17)$$

$$\text{Backward : } f(x) = \int_{-\infty}^{\infty} \hat{f}(\omega) e^{i2\pi\omega x} d\omega \quad (18)$$

where ω stands for frequency in Fourier space.

A.3. LRA Configuration Details

We tried to follow all hyperparameters as suggested for each of the attention approximations with exceptions on Linformer and Linear Trans. in Image and Pathfinder. For them, we experimented with five additional configurations as shown in Table 3.

For all fixed wavelet transform conducted in this work, we use Daubechies-2 ([Daubechies, 1992](#)) as the basis and we set the level of decomposition to 1.

For Performer, the number of random features in the random feature kernel is set as 256 for all text tasks (ListOps, Text, Retrival), 512 for all image tasks (Image, Pathfinder).

We use the same set of hyperparameters for all the attention methods on individual tasks, the detailed setting is shown in Table 4. We adjust the training length to stabilize the

WISE: Wavelet Transformation for Boosting Transformers' Long Sequence Learning Ability

Hyperparameter	ListOps	Text	Retrieval	Image	Pathfinder
Batch Size	400	128	64	64	512
Max Step	80k	50k	50k	200k	500k
Min Step	5k	20k	20k	20k	20k
Layers	8	6	6	8	1
Embedding Dim.	128	256	256	128	128
Attention Dim.	64	256	128	64	64
MLP Dim.	128	1024	256	128	128
Attention Heads	1	1	1	1	8
AdaWISE WLen.	40	16	40	40	40
OrthoWISE WLen.	16	16	16	16	16
LiftWISE Lev.	3	3	3	3	3
Dropout	0.1	0.1	0.1	0.1	0.2
Attention Dropout	0.1	0.1	0.1	0.1	0.1
Readout	CLS	CLS	CLS	CLS2	MEAN

Table 4: Hyperparameter configurations for parameterized WISE experiments.

Table 5: Evaluation results on Long-Range Arena benchmark. We show both the average accuracy (Avg) and average accuracy without Retrieval (Avg (w/r)) since LUNA 256, Nystromformer, and our WISE coupled with full attention and direct wavelet parameterization (AdaWISE-Atten) all use prolonged training steps on Retrieval.

Model	ListOps	Text	Retrieval	Image	Pathfinder	Avg	Avg (w/r)
Transformer	36.37	64.27	57.46	42.44	71.40	54.39	53.62
Local Attention	15.82	52.98	53.39	41.46	66.63	46.06	44.22
Sparse Trans.	17.07	63.58	59.59	44.24	71.71	51.24	49.15
Longformer	35.63	62.85	56.89	42.22	69.71	53.46	52.60
Linformer	35.70	53.94	52.27	38.56	76.34	51.36	51.14
Reformer	37.27	56.10	53.40	38.07	68.50	50.67	49.99
Sinkhorn Trans.	33.67	61.20	53.83	41.23	67.45	51.39	50.89
Synthesizer	36.99	61.68	54.67	41.61	69.45	52.88	52.43
BigBird	36.05	64.02	59.29	40.83	74.87	55.01	53.94
Linear Trans.	16.13	65.90	53.09	42.34	75.30	50.55	49.92
Performer	18.01	65.40	53.82	42.77	77.05	51.41	50.81
FNet	35.33	65.11	59.61	38.67	77.80	55.30	54.23
LUNA 256	37.98	65.78	79.56	47.86	78.55	61.95	57.54
Nystromformer	37.15	65.52	79.56	41.58	70.94	58.95	53.80
AdaWISE-Atten	55.4	81.6	79.27	55.58	81.12	70.59	68.42

adaptive wavelets, the training will take over min steps and then will terminate with patience ($= 10\% * \text{max step}$). We also find out that on the image task, it is better to use both the first and last output as the readout (CLS2) for parameterized wavelet transformation.

A.4. Ablation Study

We conduct an ablation study for WISE, as shown in Table 6. For (Linear), We limit the transformation in wavelet space to be linear. For (Fourier), we use the Fourier transform as the transformation mechanism for WISE. For (Forward Fourier), we only use the forward Fourier transform without backward transform. It can be observed that performance dropped significantly in all cases, indicating the necessity of non-linearity in wavelet space and forward-backward wavelet transform. For fixed WISE, we also try out different wavelet families and decomposition level when paired with Performer, results shown in Table 7. We further test the necessity of wavelets in direct wavelet parameterization scheme. We tried two other initializations on ListOps task when coupled with full attention, one with random Gaus-

Table 6: Ablation study on Long-Range Arena benchmark.

Model	ListOps	Text	Retrieval	Image	Pathfinder	Avg	Avg (w/r)
WISE	38.20	75.60	78.56	42.98	79.17	62.90	58.99
Linear	37.70	55.36	55.27	15.75	50.58	42.93	39.84
Fourier	36.85	65.52	60.56	9.99	50.49	44.68	40.71
Forward Fourier	37.15	64.91	65.98	37.84	53.39	51.85	48.32

Table 7: Ablation study for different wavelet families & decomposition levels for fixed WISE-Performer on Long-Range Arena benchmark.

Config	ListOps	Text	Retrieval	Image	Pathfinder
Daubechies-2, L=1	38.20	75.60	78.56	42.98	79.17
Daubechies-3, L=1	37.85	76.86	73.62	42.30	78.30
Daubechies-3, L=2	37.40	76.84	75.43	41.20	50.52
Coiflet-1, L=1	36.85	76.72	75.43	41.42	50.58
Coiflet-1, L=2	37.65	75.97	75.29	43.2	77.49
Symlet-2, L=1	37.50	75.07	75.59	42.85	49.85
Symlet-2, L=2	37.45	75.63	74.51	41.03	77.39
Symlet-2, L=3	37.55	75.39	76.24	40.88	76.84

sian initialization $N(\mu = 0, \sigma = 0.02)$, the other one with damped sinusoidal wave initialization. It can be observed from Table 8 that both alternative initializations induced significant performance deterioration.

Table 8: Ablation study for Daubechies wavelet initialization, Gaussian initialization, and damped sinusoidal wave initialization. All experiments are using full attention as the non-linearity.

Initialization	ListOps
Daubechies init.	55.4
Gaussian init.	45.9
Damped Cos init.	44.65